Journal of Marine Research, 52, 297–323, 1994

Aggregation and sedimentation processes during a spring phytoplankton bloom: A field experiment to test coagulation theory

by Thomas Kiørboe[1], Claus Lundsgaard[2], Michael Olesen[2] and Jørgen L. S. Hansen[2]

ABSTRACT

Spring diatom blooms in temperate waters are often terminated by aggregation of the cells into large flocs and subsequent mass sedimentation of the phytoplankton to the sea floor. The rate of aggregate formation by physical coagulation depends on the concentration of suspended particles, on the turbulent shear that makes particles collide, and on their stickiness (= probability of adhesion upon collision). During a mixed diatom bloom in a shallow Danish fjord, for 3 weeks we monitored the concentration and stickiness of suspended particles and the species composition of the phytoplankton at 2–3 d intervals and we estimated the turbulent shear rate from observations of wind velocity. By means of coagulation theory these observations were combined into a predictor of aggregation rate. We also quantified the sedimentation of phytoplankton, other suspended particles and of aggregates by means of moored sediment traps. The sinking velocity of suspended particles and the sedimentation of aggregates varied in concert during the 3-week period and were closely mimicked by the coagulation-based predictor of aggregate formation. The population dynamics of the five quantitatively significant diatom species were all similar. During the first week of observation all increased approximately exponentially in abundance; thereupon the populations fluctuated around species-specific concentrations (10^0 – 10^4 cells ml^{-1}), even though nutrients were not limiting their growth. This pattern is consistent with a simple coagulation model of Jackson (1990), according to which growth and coagulation (and subsequent sedimentation) will balance at a certain equilibrium concentration. The equilibrium concentrations observed were accurately predicted by the model, and the stickiness coefficients estimated by the model were in accordance with those reported in the literature. Thus, aggregate formation by coagulation appears to account for the vertical flux of particles and for the dynamics of the diatom bloom in the fjord studied.

1. Introduction

Spring diatom blooms in temperate, coastal waters are often assumed to sediment out of the water column rather than being grazed by planktonic heterotrophs, and flocculation of diatoms into large, rapidly sinking aggregates has been implicated as

1. Danish Institute for Fisheries and Marine Research, Charlottenlund Castle, DK-2920 Denmark.
2. Marine Biological Laboratory, DK-3000 Helsingør, Denmark.

an important mechanism facilitating the phytoplankton fallout (Smetacek, 1985). Observations of abundant phytoplankton aggregates at the height of diatom blooms support this view (Kranck and Milligan, 1988; Alldredge and Gotschalk, 1989; Riebesell, 1991 a,b; Olesen, 1993).

Aggregation of phytoplankton may take place by various mechanisms, e.g. by packaging of algal cells into fecal pellets or by coagulation. Coagulation is a process by which particles collide due to interparticle velocity differences and subsequently stick together. Theoretical models have suggested that coagulation may be an important aggregation mechanism during phytoplankton blooms, where the concentration of phytoplankton is high and the abundance of grazers is low (Jackson, 1990; Jackson and Lochmann, 1992, 1993; Hill, 1992).

According to classical coagulation theory, aggregation of suspended particles depends on the concentration of particles, the size of the particles, the turbulent shear rate that makes particles collide, and on their stickiness (= the probability of sticking upon collision) (Smoluchowski, 1917; McCave, 1984). Other processes may bring about collisions between suspended particles, particularly differential settling, but these have (initially) been ignored in the present account. In principle, then, provided the above parameters and processes can be quantified, it is possible to predict the aggregation and subsequent sedimentation of particles and phytoplankton due to coagulation.

The aim of the present study has been to describe the development and fate of a diatom spring bloom in the shallow Isefjord (Denmark) and specifically to evaluate the importance of physical coagulation for the sedimentation of the phytoplankton. The approach taken here has been (i) to monitor during a spring phytoplankton bloom the concentration and size distribution of suspended particles and phytoplankters, the turbulent shear rate (estimated from wind velocity) and the stickiness of suspended particles; (ii) from this to come up with semiquantitative predictions of *in situ* aggregate formation; and (iii) to compare the predicted temporal pattern in aggregate formation to the observed temporal patterns in sedimentation of aggregates and sinking velocities of suspended particles. We show that aggregate formation plays a major role in the sedimentation of suspended matter and that the temporal development of the spring diatom bloom as well as patterns in sedimentation can be largely accounted for by coagulation theory.

2. Material and methods

Sampling was conducted at a station (bottom depth of 10 m) in the northeastern part of Isefjord (Fig. 1) from R/V *Ophelia.* Isefjord is a eutrophic, brackish fjord. The average, maximum and sill depths are 7, 17 and 3 m, respectively. The fjord receives freshwater from several small rivers as well as from diffuse drainage and connects to the open sea (Kattegat) in the north. Annual freshwater inflow (133×10^6 m^3) corresponds to about 10% of the fjord's water volume (1560×10^6 m^3), and annual

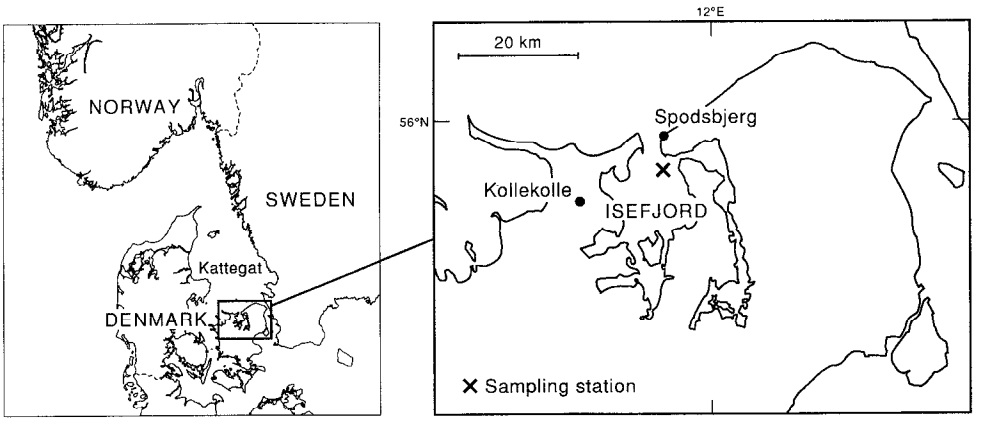

Figure 1. Map of study area with position of sampling station and meteorological stations.

precipitation almost balances evaporation (145×10^6 and 180×10^6 m^3, respectively). The salinity is relatively constant (18–22‰), and water residence time is high, 3 months during winter and 12 months during summer. Entrance of water across the sill occurs mainly as episodic intrusions of saline water from the Kattegat during periods of strong winds from the sector NE-S. These intrusions become evident as episodic salinity stratifications of the fjord. (Anon., 1973; 1989).

Sampling was carried out about 3 times per week between February 24 and March 18. This is the expected timing of the spring diatom bloom. On each sampling occasion we measured vertical profiles of salinity and temperature (Salinity-Temperature Bridge, Type M.C.5, Electronic Switchgear Ltd., London) and *in situ* fluorescence (Q-Instruments fluorometer, Copenhagen).

Water samples (30 l Niskin bottle) were collected at 3–5 depths to quantify the concentration of inorganic nutrients (autoanalyzer) and to quantify and characterize the suspended particulate matter.

a. Suspended particles and primary production

Samples for determination of pigments were filtered onto GF/C filters and extracted in 96% ethanol (Jespersen and Christoffersen, 1987). Chlorophyll *a* and phaeopigments were measured with a method based on Lorenzen (1967), using an acid factor of 1.7 and an absorption coefficient of 83.4 g $cm^{-1}l^{-1}$ (Wintermans and DeMots, 1965).

The volume fraction of suspended particles in the size range 3–78 μm equivalent spherical diameter (ESD) was measured on an electronic particle counter (ELZONE 180, Particle Data, Inc.) equipped with a 120 μm orifice tube. Particulate organic carbon and nitrogen (POC and PON) were measured by a CHN analyzer (Carbo Erba Instruments, E.A. 1108) on material filtered onto muffled GF/C glassfibre filters. Phytoplankton species composition and concentration were quanti-

fied by inverted microscopy in 50–175 ml samples; *Skeletonema costatum* was counted in 9% of the sample volume, while all cells of other species were counted. Large and numerically rare species (*Coscinodiscus concinnus*) were quantified in 2 l samples that were concentrated on a 100 μm plankton mesh. Biovolumes were estimated from measurements of linear dimensions assuming simple geometrical shapes, and carbon content was calculated from species specific carbon to volume ratios (Edler, 1979).

Phytoplankton primary production was measured as ^{14}C fixation. Water from three depths was incubated *in situ* for 3 h in 58 ml glass bottles added 3 μCi $NaH^{14}CO_3$. We had one light and one dark bottle at each depth. After incubation one 0.50 ml sample for total ^{14}C ($T^{14}C$) and two 10.00 ml samples for total organic ^{14}C ($TO^{14}C$) determinations were taken from each bottle. $T^{14}C$ samples were added 0.5 ml metoxy ethylamine in a scintillation vial. TOC samples were acidified to pH 2.5–3 with 1 N HCl and allowed to stand in open scintillation vials for at least 24 h to remove inorganic carbon. Instagel (Packard) was added to the vials and disintegrations per minute were measured in a Packard 1500 scintillation counter. Water samples were analyzed for inorganic carbon (TIC) on an IRGA. The carbon fixation was calculated as: TIC × $TO^{14}C/T^{14}C$. Photosynthetic carbon fixation was corrected for dark fixation. To calculate the daily primary production the carbon fixation m^{-2} was divided by the photosynthetically active radiation (PAR) in the incubation period and multiplied by PAR from the whole day. Light was measured continuously at the nearby (50 km) laboratory and during incubations also on the ship.

b. Sedimentation and sinking velocities of suspended particles

Sediment traps were deployed for measuring sedimentation at each sampling occasion. Cylindrical sediment traps with a diameter of 5.3 cm and an aspect ratio of 6.4 were used (Olesen, 1993). The traps were deployed at 3 or 4 depths (3, 5, 7 and 9 m or 4, 6, and 8 m) on an anchored mooring for ca. 4 hours at each sampling occasion (short time deployments, STD) and for 24–72 h (and up to 120 h) between the sampling occasions (long time deployments, LTD). We had three STD and 3 LTD traps per depth. No preservatives were used in the traps.

After the traps were picked up the supernatant water in the cylinders was removed. Subsamples of the sedimented material were taken from two STD and two LTD traps for analysis of POC, PON and chlorophyll *a* as described above, except that in STD traps chlorophyll was determined fluorometrically (Strickland and Parsons, 1968) after intercalibration of spectrophotometer and fluorometer. In LTD traps from one depth (4 or 5 m) subsamples (0.4%) for cell counts were preserved with 1% Lugols solution and with 1% glutaraldehyde (final concentrations). All cells were counted (inverted microscope), except *Skeletonema costatum,* that was counted in only 4% of the subsample volume. From the same depth all sedimented material in

one trap was washed on a 100 μm plankton mesh and *Coscinodiscus concinnus* cells were counted.

In the bottom of one of the STD traps at 4 or 5 m depth we placed a petri dish filled with a viscous acrylamide polymer solution to collect aggregates (Jannasch *et al.*, 1980). The polymer conserves the 3-D structure of the aggregates, and prevents further aggregation in the trap. Upon retrieval, the petridish was photographed, and aggregates >0.5 mm at the longest dimension were characterized, counted and measured (linear dimensions). The volume of individual aggregates was calculated assuming simple geometrical shapes.

The average sinking velocity [m d^{-1}] of POC, PON and chlorophyll *a* was calculated as: sedimentation rate [mg $m^{-2}d^{-1}$] divided by the concentration [mg m^{-3}] in the surrounding water at the same depth. For LTD traps the average concentration at time of deployment and pick up was used in this calculation.

c. Stickiness and flocculation index of suspended particles

Large volumes (50 l) of water were collected in the middle of the water column on every sampling day and transported to the laboratory. Here the samples were passed though a 100 μm screen and the stickiness (= probability that particles will stick upon collision) of suspended particles (< 100 μm) was assessed by allowing particles to aggregate in a Couette device as described by Kiørboe and Hansen (1993). The Couette device consists of two closed, concentric cylinders (radii 4.35 and 5.65 cm, length 24.9 cm); by allowing the outer cylinder to rotate well defined laminar shear is generated in the water-filled annular gap between the cylinders (Duuren, 1968). All experiments were run at a shear rate of 30 s^{-1}. In several instances the naturally occurring particles were concentrated by inverse filtration through a 11 μm plankton net and the flocculation of the >11 μm particles was also investigated. We had 4 Couette incubators and, therefore, 2 or 4 replicates of each treatment. We monitored the decline in particle concentration in the Couette cylinders by an electronic particle counter. The cylinders were sampled at 0, 15, 30, 60, 90, 120, 150 and ca. 1200 min.

The stickiness (α) of suspended particles was estimated by regressing $\log_e$ particle concentration vs. incubation time in the Couette device according to (Kiørboe *et al.*, 1990):

$$C_t = C_0 \exp^{-(7.824\alpha\phi\gamma/\pi)t} \quad (1)$$

where ϕ is the volume fraction of suspended particles and γ is the laminar shear rate in the Couette cylinder. Since α is the only unknown in the above equation, it can be solved for.

Flocculation was also quantified by monitoring the change in particle size distribution over time by means of a laser diffraction instrument (MALVERN). By laser diffraction the particle volume (including 'interstitial' water) distribution is mea-

sured. It can be shown that the average diameter (L) of particles initially will increase approximately according to:

$$L^D = Ke^{(7.824\alpha\phi\gamma/\pi)t} \tag{2}$$

where K is a constant and D is the fractal dimension of the aggregates. As a measure of L we used the 50% fractile of the cumulative volume distribution rather than the average (by number) particle diameter. This is because laser diffraction yields much 'noise' in particle numbers in the lower size channels. The 50% fractile of the volume distribution is some power function of the average particle size, depending on the actual size distribution. Also, since the volume distribution develops into a bimodal distribution as flocculation proceeds (with peaks representing aggregates and nonaggregated particles) this is a crude estimate of particle size. Due to these inaccuracies but inspired by Eq. 2 we define a flocculation index:

$$\text{Flocculation index} = \text{'slope'}/\phi \tag{3}$$

where 'slope' is the slope of a regression of $\log_e L$ (50% fractile) vs. incubation time. Although this approach is not strictly quantitative it does provide a semiquantitative index of how readily the suspended particles flocculate. The advantage of laser diffraction over electronic particle counting to analyze particle size distributions is that aggregates are not disintegrated by the laser beam, as they potentially are when accelerated through the orifice of the electronic particle counter.

d. Laboratory incubations

On two occasions (Feb. 27 and 28) an additional 85 l of water, collected as above, were incubated in 100 l tanks in the laboratory at approximately *in situ* temperature (5°C) and light (L:D = 12h:12h; ca. 80 μE $m^{-2}s^{-1}$). Prior to incubation the water was passed through a 180 μm sieve to remove larger zooplankters. To avoid settling of particulate material the tanks were vigorously aerated. One to four times per day the tanks were sampled for measurements of inorganic nutrients, particulate chlorophyll, carbon and nitrogen (as above), in vivo fluorescence (Aminco Fluorocolorimeter) and phytoplankton species composition.

e. Wind and turbulent shear

Records of wind velocity were obtained from two meteorological land stations (Spodsbjerg Fyr and Kollekolle) close to the sampling station (Fig. 1). Wind velocities were measured during four (Spodsbjerg) and three (Kollekolle) 10-min periods between 9 am–3 pm and 8 am–9 pm, respectively. Since wind velocities at the two stations were similar and strongly intercorrelated (r^2 = 0.81), all observations were pooled into one daily average.

Daily average turbulent energy dissipation rates (ϵ, m^2 s^{-3}) in the 10 m water column due to winds were estimated from wind velocity by applying the empirical

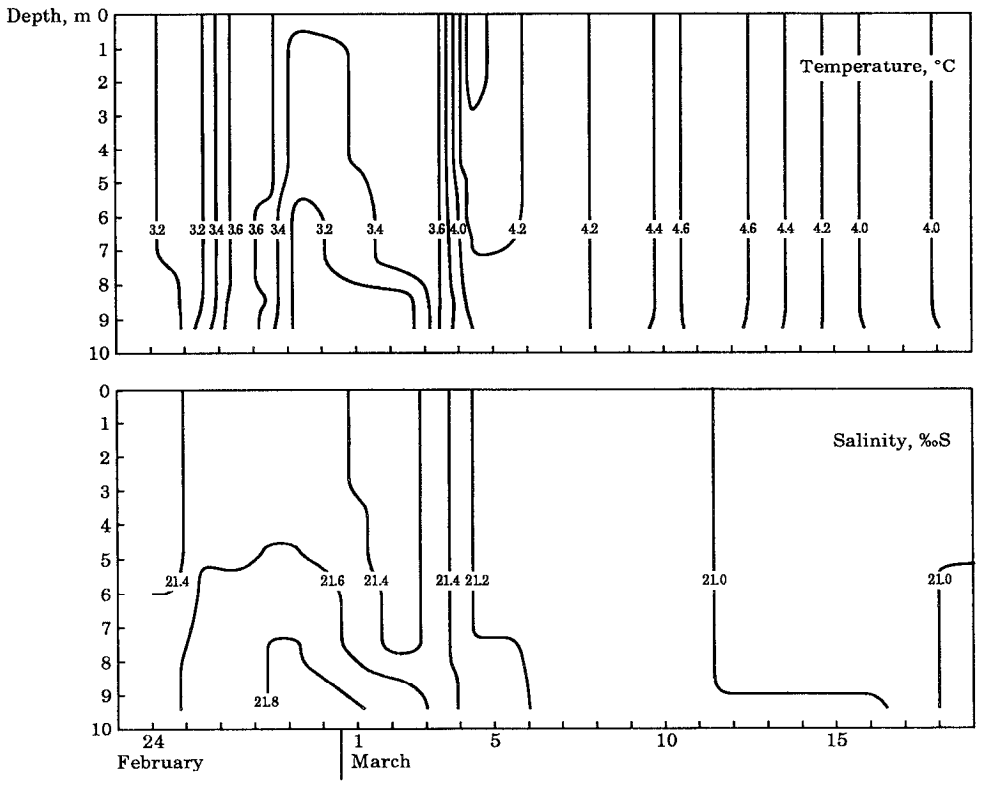

Figure 2. Isopleth diagrams of (a) salinity and (b) temperature at the sampling station between February 24–March 18.

wind-ϵ regression model for shelf seas of MacKenzie and Leggett (1991). Average fluid shear rates (γ, s^{-1}) were subsequently calculated from $\gamma = (\epsilon/\nu)^{0.5}$ (Camp and Stein, 1943), where ν is the kinematic viscosity ($10^{-6} m^2 s^{-1}$).

3. Results

a. Physical and chemical observations

i. Salinity and temperature. Isopleth diagrams of salinity and temperature (Fig. 2) show very weak or nonexisting vertical stratification of the water column. The salinity declined only slightly (from 21.6 to 20.8, water column average), suggesting that no major intrusions of water from the Kattegat occurred, and that horizontal advection was minimal (i.e. restricted to advection of homogeneous fjord water over the sampling station) during the observation period. This is also supported by the fact that the wind direction during periods of stronger winds (see below) were from SW–NW; winds from these directions do not normally give rise to intrusions of Kattegat water into the fjord.

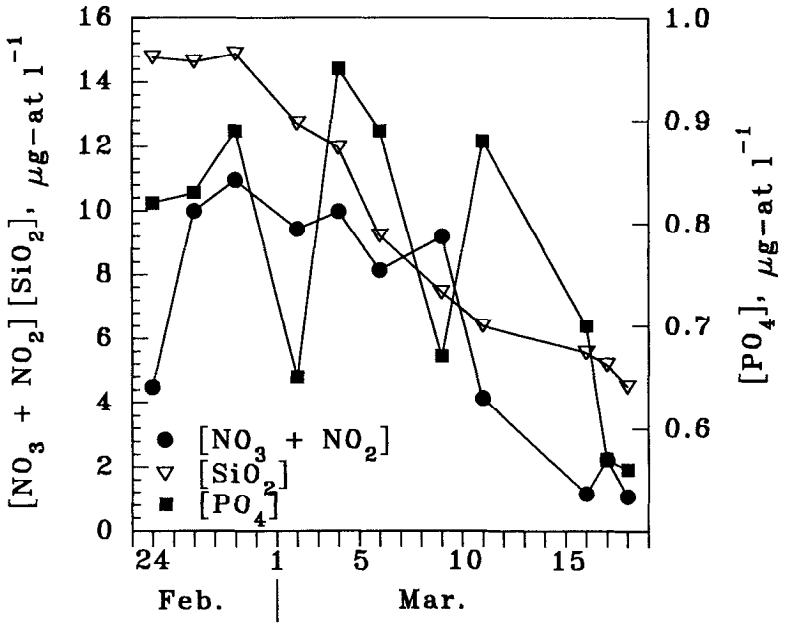

Figure 3. Concentration of inorganic nutrients (depth-averaged) at the sampling station.

ii. Inorganic nutrients. There was no vertical variation in nutrient concentrations and the concentrations of nitrite + nitrate, phosphate and silica never fell below 1, 0.5 and 4 μg-at/l (depth-averaged values, Fig. 3), respectively. Thus, nutrients probably did not become limiting for phytoplankton growth during the observation period.

iii. Wind and shear. There were three wind events during the observation period with daily average wind velocities exceeding 7.5 m s^{-1}; viz. on Feb. 23 immediately before sampling commenced, on March 2–3 and a longer period between March 9–16 with peak winds March 12–14 (Fig. 4a).

Calculated fluid shear rates of course followed wind velocities (Fig. 4b). Average shear rate for the entire observation period was 1.2 s^{-1} and during periods of elevated wind estimated shear rates exceeded 2–3 s^{-1}. Given such high rates it is likely that shear rather than differential settling, at least initially, is the dominating process in bringing suspended particles to collide (McCave, 1984).

b. Development of the spring bloom and composition of suspended matter

i. Chlorophyll and primary production. There was limited vertical structure in the distribution of chlorophyll. Thus, depth-averaged concentrations of chlorophyll are representative for the temporal development of the spring phytoplankton bloom (Fig. 5). From the start of the observation period, Feb. 24, until March 11 the chlorophyll biomass increased approximately exponential, whereupon it was almost

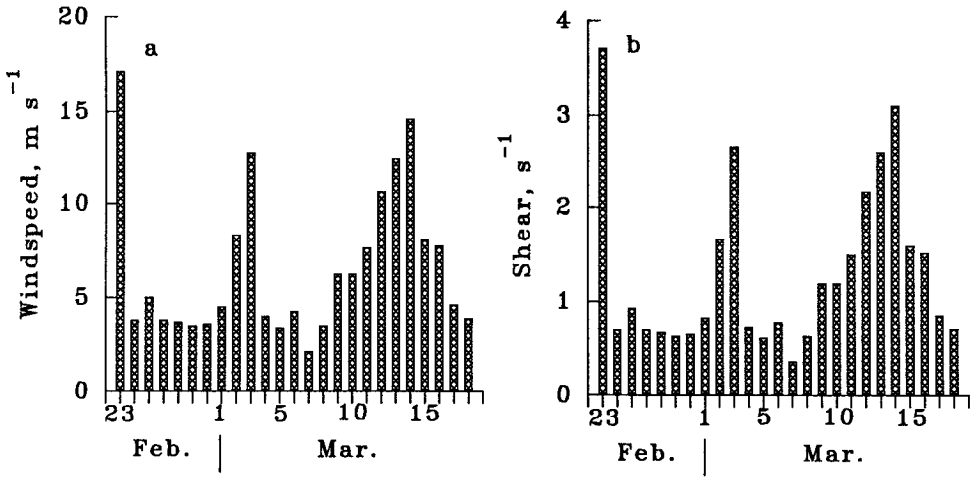

Figure 4. Daily average wind velocities (a) and calculated turbulent fluid shear (b) at the sampling station.

constant until the end of the period. During the period of increase, the exponential rate of net increase was 0.10 d^{-1} (r^2 = 0.81).

The temporal development of primary production (Fig. 5) largely followed the concentration of chlorophyll, and the assimilation number (= ratio of primary production to concentration of chlorophyll) varied by less than a factor of 2, between 4.9–9.7 μg C d^{-1} (μg Chl)$^{-1}$. Thus, phytoplankton growth was relatively constant throughout the observation period and showed no sign of nutrient limitation.

ii. Volume fraction of suspended particles (3–78 μm ESD). The volume concentration of suspended particles varied in concert with chlorophyll concentration (Fig. 6a), and

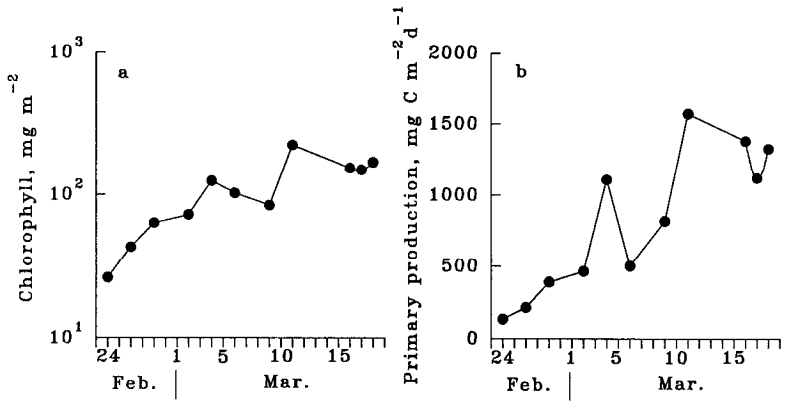

Figure 5. Biomass of chlorophyll *a* (a) and rate of primary production (b) at the sampling station.

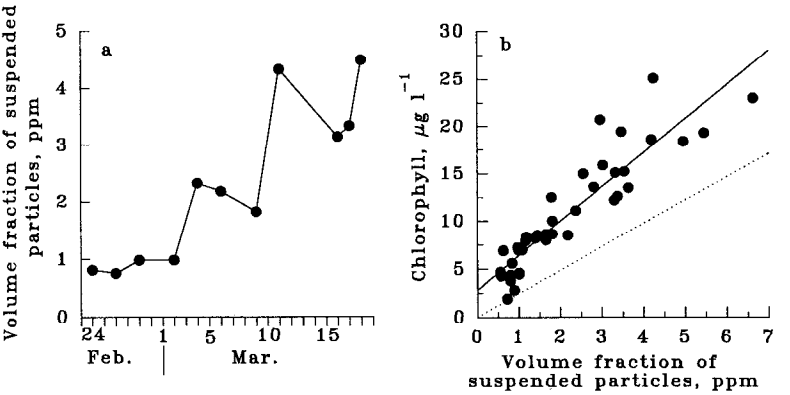

Figure 6. Temporal variation of the volume fraction of suspended particles in the size range 3–78 μm equivalent spherical diameter (depth-averaged) (a) and relation between the concentration of particulate chlorophyll (CHL) and volume fraction of suspended particles (VFS) (b). The full line in (b) is the regression line: CHL = 2.83 + 3.60 VFS (n = 40, r^2 = 0.83). The dotted line is the expected relationship assuming all particles to be phytoplankters, C:Chl = 45 and 0.11 × 10^{-6} μg C μm^{-3}.

the two were intercorrelated (Fig. 6b). This suggests that suspended particle biomass was dominated by phytoplankton. In fact, the volume fraction of suspended particles (3–78 μm) was insufficient to account for observed chlorophyll biomasses in that most observations of chlorophyll were higher than those predicted from particle volume by assuming C:Chl = 45 and 0.11 × 10^{-6} μg C μm^{-3} (see dotted line in Fig. 6b). This is due to the occurrence of >78 μm phytoplankters (i.e. *Coscinodiscus concinnus*).

iii. POC and PON. The variations in POC and PON followed the concentration of suspended chlorophyll, again suggesting that the majority of suspended material was phytoplankton. Plots of POC and PON vs. chlorophyll yield linear relationships (Fig. 7), and C:Chl and N:Chl ratios of 45.8 and 7.2 can be estimated. This implies a phytoplankton C:N-ratio (by weight) of 6.4, which is close to the Redfield ratio. Intercepts of 99 μg l^{-1} POC and 16 μg l^{-1} PON suggest non-algal background concentrations on this order of magnitude.

iv. Phytoplankton species composition. The phytoplankton community was numerically dominated by *Skeletonema costatum* throughout the study period and this species reached concentrations of 10^4 cells ml^{-1} (Fig. 8). The diatoms *Thalassiosira* spp. (predominantly *T. nordenskjoldii*), *Leptocylindrus danicus* and *Rhizosolenia hebetata f. semispina* as well as the autotrophic ciliate *Mesodinium rubrum* were all 2–3 orders of magnitude less abundant, and the diatom *Coscinodiscus concinnus* 4 orders of magnitude less abundant (Fig. 8). Initially all diatom species increased

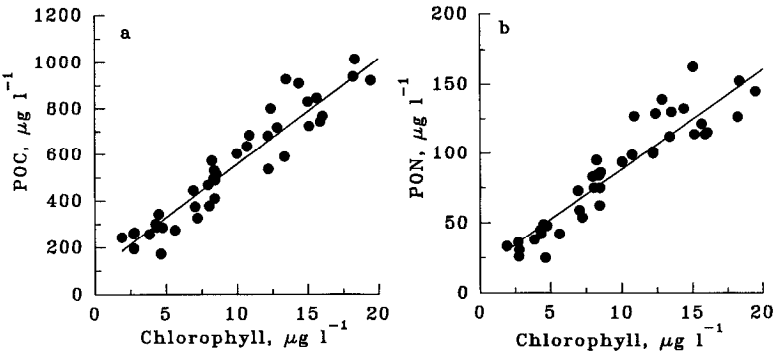

Figure 7. The relationships between suspended particulate organic carbon (POC) and chlorophyll *a* (CHL) (a) and suspended particulate organic nitrogen (PON) and chlorophyll *a* (b). The regressions are: POC = 45.8 CHL + 99.3 (n = 41, r^2 = 0.90) and PON = 7.22 CHL + 16.3 (n = 41, r^2 = 0.86).

approximately exponentially in abundance, with net population growth rates during the first 3–4 observation days of between 0.25 – 0.54 d^{-1} (Table 2); population growth rates varied independently of cell sizes. Subsequently population sizes fluctuated around more or less constant, species-specific concentrations during the remainder of the observation period. These fluctuations were to some extent synchronized between species; for example, all diatom species temporarily declined in abundance after March 4, subsequent to the wind event March 2–3.

v. Phytoplankton development in tank experiments. Skeletonema costatum made up >80% of the phytoplankton biomass in both tanks throughout the experiment. The *S. costatum* populations initially increased exponentially with a growth rate of ca. 0.5 d^{-1}. Population growth rate ceased when or slightly after nutrients were exhausted (either phosphate or silicate), and cell concentration in the stationary phase was about 60,000 cells ml^{-1}, ca. 10 times higher than for the field population. The continued dominance of *S. costatum,* the higher net growth rate and the higher maximum concentration in the laboratory tanks compared to the field situation together suggest that factors limiting *S. costatum* in the field were not operating in the tanks. Since zooplankters were removed and flocculation did not occur (due to strong aeration) in the tanks, grazing and/or flocculation and sedimentation may be the factors responsible.

c. Stickiness and flocculation index of suspended particles

Stickiness and flocculation index of the assemblage of suspended particles as they developed during the study period have been plotted in Figure 9. Except for a high flocculation index measured on March 16, the two measures followed the same temporal pattern (α vs. $\log_e$ flocculation index, omitting March 16: r^2 = 0.65, n = 9,

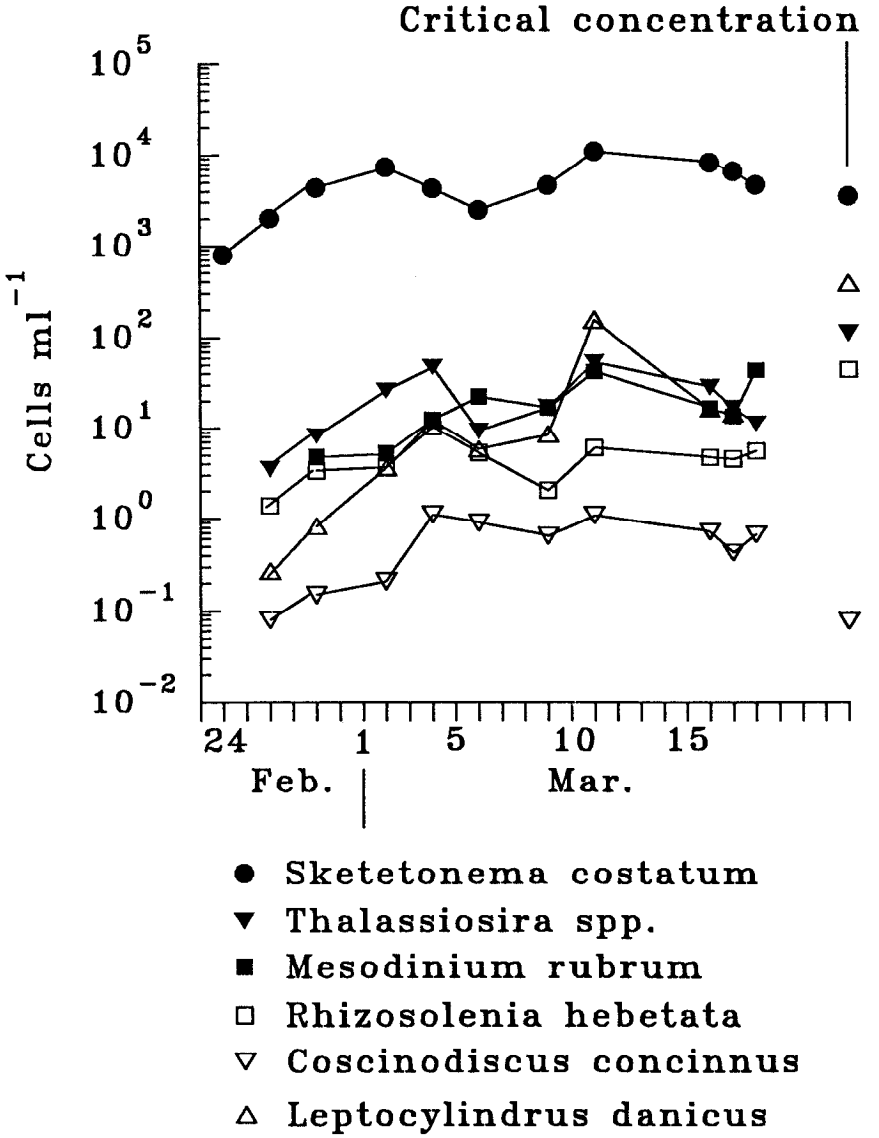

Figure 8. Cell concentrations of dominating phytoplankton species during the observation period. *Thalassiosira* spp. is predominantly *T. nordenskjoldii.* Estimated 'critical concentrations' for each of the diatom species have also been shown; see text for further explanation.

$p < 1\%$); i.e., high in the beginning of the study period and declining to lower values after March 2. The high flocculation index measured on March 16 is real, since it was confirmed by visual and microscopic examination, but was not reflected by the stickiness coefficient, α, because formed flocs were very fragile on this day and disintegrated during electronic particle counting.

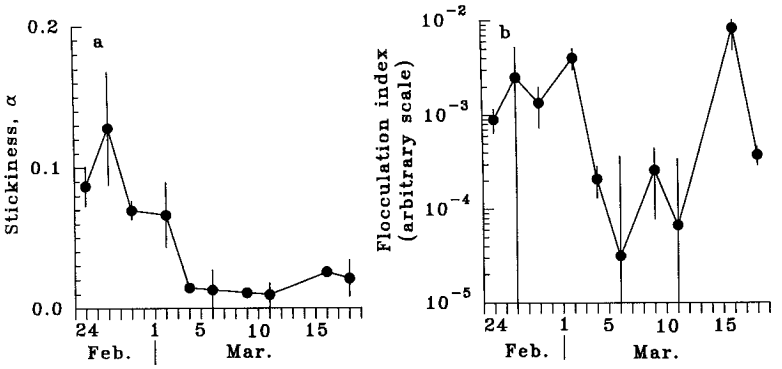

Figure 9. Estimated stickiness (α) (a) and flocculation index (b) of naturally occurring particles at the sampling station. Bars are ± SD.

After March 2 flocculation was also quantified in water samples in which particles >11 μm had been concentrated by inverse filtration. The flocculation indices in concentrated and untreated samples were significantly correlated ($r^2 = 0.89$, $n = 7$, $p < 0.2\%$) and yielded similar temporal patterns. This was also more or less the case for the estimated particle stickiness coefficients ($r^2 = 0.40$, $n = 7$, $t = 1.89$), except for one instance. On March 4 we observed strong flocculation in the upconcentrated samples during the first 60 min of observation. Analyzing data for $t = 0$–60 min separately yielded $\alpha = 0.60$.

All samples taken in the Couette incubators for analysis of particle concentration and -size distribution were also examined microscopically (inverted microscope). In general there was a good correspondence between microscopic observations and the above quantitative measures of flocculation. That is, when changes in size distribution during Couette-incubations suggested flocculation we also observed flocs microscopically. Frequently flocs were also evident by the naked eye. *S. costatum* and other diatoms always contributed to these flocs, but so did unidentifiable particles ('detritus') to a varying extent. On Feb. 28, March 2 and particularly on March 4 flocs formed in the Couette incubators were entirely dominated by cells (and chains) of *S. costatum.* To what extent flocculation was caused by algal-algal, detritus-detritus or algal-detritus sticking cannot be decided from these observations, and estimated particle stickiness and flocculation index refer to the average properties of the entire particle assemblage.

d. Sedimentation and sinking rates of particulate material

i. Long term deployments. Sedimentation rates for particulate carbon (POC), nitrogen (PON) and chlorophyll have been plotted in Figure 10a–c. Figures shown are averages for the 3–4 traps deployed during each period as there were no significant vertical differences in sedimentation. All parameters showed approximately the same temporal pattern in sedimentation, with elevated sedimentation rates on

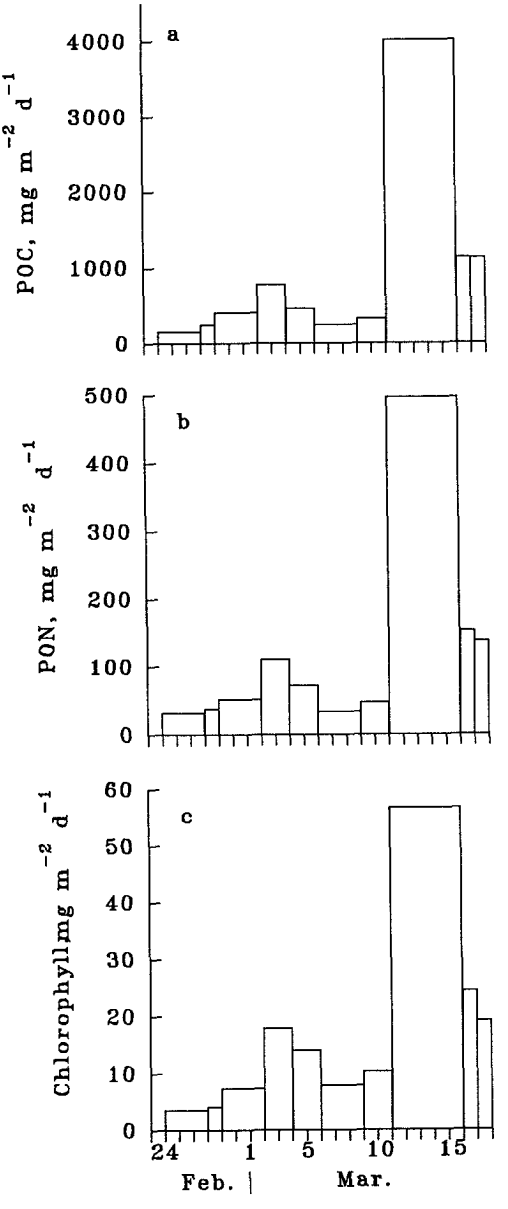

Figure 10. Sedimentation rates (depth-averaged) in long term deployment traps (LTD) of (a) particulate organic carbon (POC), (b) particulate organic nitrogen (PON) and chlorophyll *a* during the observation period.

March 2–4, March 11–16, and high rates also during March 16–18. Sedimentation events, thus, coincided or occurred immediately subsequent to wind events.

Bulk properties of the sedimented material resembled that of the suspended matter; for example, both the POC and the PON vs. chlorophyll *a* relationships were

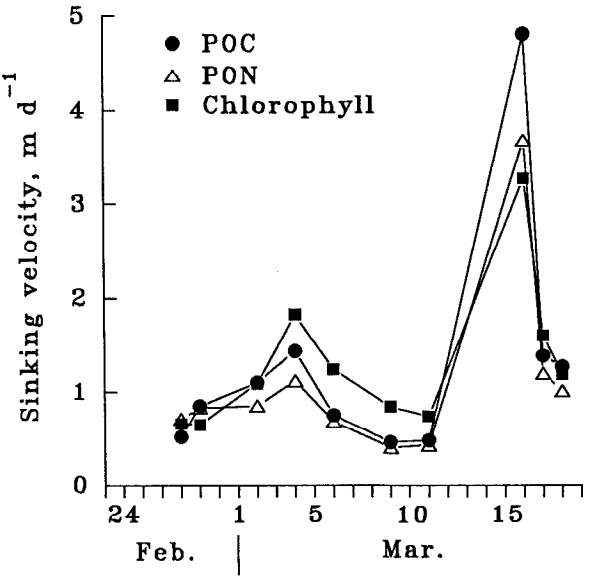

Figure 11. Sinking velocities calculated from LTD-traps (averages of 3–4 sediment trap depths) of particulate organic carbon (POC), particulate organic nitrogen (PON) and chlorophyll *a*. Sinking velocities are integrated averages over the deployment periods (see Fig. 10).

linear (r^2 = 0.81 and 0.86, respectively) and yielded C:Chl, N:Chl and C:N ratios of 43.6, 6.0 and 7.3, respectively. This is not significantly different from the corresponding ratios of suspended matter.

Sinking velocities of POC, PON and Chlorophyll (Fig. 11) were similar and varied in concert during the observation period. Sinking velocities were ca. 0.5 m d^{-1} until March 2, about 2 m d^{-1} March 2–4, low ($<$1 m d^{-1}) again until March 11, and very high, 4–5 m d^{-1}, during March 11–16. There were, thus, two events of elevated sinking velocities during the observation period, and both were associated with elevated wind velocities. In comparison, sinking velocities of unaggregated fluorescent particulate matter measured in water samples transported to the laboratory, consistently yielded values between 0.35–0.45 m d^{-1} between March 2–18 (unpublished observations).

Sinking velocities for individual algal species were very variable and for rare species no consistent patterns emerged. Sinking velocities of *Skeletonema costatum* and *Coscinodiscus concinnus* have been shown in Figure 12. *S. costatum* showed elevated sinking velocities, up to 3 m d^{-1}, between Feb. 28 and March 6 and *C. concinnus* a peak on March 4, 7.5 m d^{-1}. Sinking velocities of both species were also elevated at the end of the observation period. Thus, the temporal pattern in sinking velocities of these two species largely resembled that of bulk particulate matter.

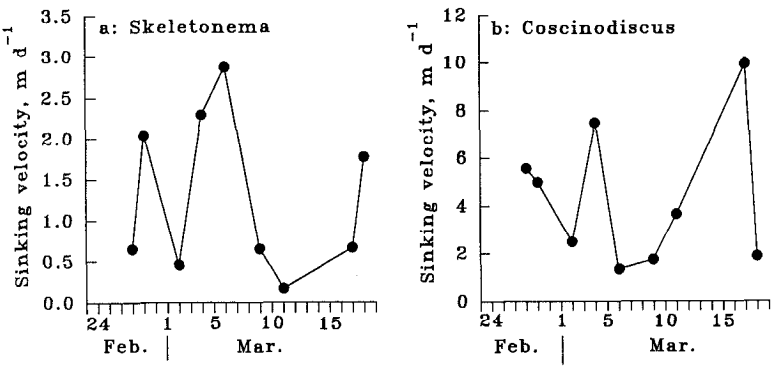

Figure 12. Sinking velocities of *Skeletonema costatum* (a) and *Coscinodiscus concinnus* (b) as calculated from LTD-traps.

ii. Short term deployments. Short term deployments of sediment traps gave the same overall pattern in sedimentation rates for POC, PON and chlorophyll as the long term deployments (Fig. 13). Sinking velocities of suspended particles derived from STD yields instantaneous rates (in contrast to time-averaged rates from LTD). The temporal variation in sinking velocities was similar to that provided by LTD, except that elevated rates were also recorded on February 24 by STD (Fig. 13). This may be a tail effect of the wind event on February 23, and appears to have had little influence on the average sinking velocity between February 24–27.

Aggregates >0.5 mm collected in the polymer in STD traps consisted of two distinct types: (1) optically dense aggregates composed mainly of detritus but with diatom cells entangled, and (2) optically less dense aggregates dominated by diatoms. Average sizes and sedimentation rates of the two types of aggregates have

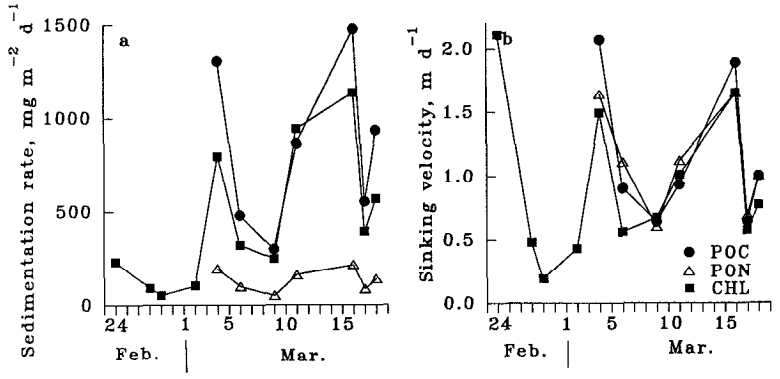

Figure 13. Short term deployment traps (STD): sedimentation rates (a) and sinking velocities (b) of particulate organic carbon (POC), particulate organic nitrogen (PON) and chlorophyll *a*. Figures are averages from 3–4 sediment trap depths. In (a) chlorophyll *a* has been converted to carbon units by multiplication with 45.

Table 1. Sedimentation and average volume of detritus- and algal aggregates (>0,5 mm in longest dimension) in STD-traps.

Date	Sedimentation of detritus aggregates, $cm^3\ m^{-2}\ d^{-1}$	Sedimentation of algal aggregates, $cm^3\ m^{-2}\ d^{-1}$	Average volume of detritus aggregates, mm^3	Average volume of algal aggregates, mm^3
24/2	21.66	0	6.05	
2/3	0.11	0	0.05	
4/3	0.73	113.35	0.27	42.47
6/3	1.11	0	0.49	
9/3	0.97	0	0.34	
11/3	1.05	0	0.43	
16/3	1.35	21.20	0.51	8.10
17/3	1.10	2.07	0.44	0.82
18/3	0.77	0.59	0.34	0.26

been given in Table 1. Sedimentation of detritus aggregates was high on Feb. 24, subsequent to strong winds on Feb. 23, and the aggregates were large. On March 2 sedimentation of detritus aggregates was limited, and the aggregates were small. During the rest of the observation period, sedimentation and size of detritus aggregates was almost constant. We observed phytoplankton aggregates on only four observation days, viz. March 4 and 16–18. The sedimentation rates of phytoplankton aggregates on March 4 and 16, immediately subsequent to strong winds, were 1–2 orders of magnitude higher than sedimentation of detritus aggregates, and the aggregates were very large, particularly on March 4. On this day dense concentrations of huge flocs were also observed by the naked eye from the boat. These observations of aggregate sedimentation are consistent with the temporal variation in settling velocities of particulate material (Figs. 11–13; see also Fig. 16 below).

4. Discussion

a. The origin of sedimented material

The cumulated sedimentation of particulate organic carbon during the entire observation period was 28.4 g C m^{-2} and the net increase in suspended POC was 6.8 g C m^{-2}. During the same period the cumulated pelagic primary production was only 19.2 g C m^{-2}. Thus, the primary production can account for only a little more than half the sum of sedimentation and pelagic accumulation of particulate carbon. This suggests that, overall, resuspension and subsequent sedimentation of POC is significant at the study site. We can estimate the sedimentary losses of phytoplankton by comparing the net accumulation rate of phytoplankton in the water column to (i) the decline in silica concentration and to (ii) the specific growth rate of the phytoplankton (from ^{14}C fixation). First, between Feb. 24 and March 11 the ratio between the amount of phytoplankton (as chlorophyll) that had accumulated in the water column

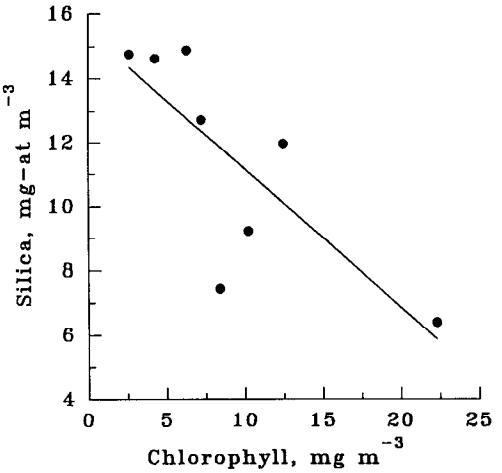

Figure 14. Depth-averaged concentration of silica (Si) as function of depth-averaged concentration of chlorophyll *a* (Chl) between February 24 and March 11. The regression is: Si = 15.48 − 0.43 Chl (n = 8, r^2 = 0.60).

and the amount of silica that had disappeared during the same period (Fig. 14) was 0.43 μg-at. Silica (μg Chl)$^{-1}$ = 12 μg Si (μg Chl)$^{-1}$. Assuming a phytoplankton C:Chl ratio of 45, this yields 3.75 μg Phytoplankton-carbon (μg Silica)$^{-1}$. In *Skeletonema costatum* the C:Silica weight ratio is about 5.5 (Own unpublished observation). If this ratio is representative for diatoms, and because diatoms (and *S. costatum*) dominate the chlorophyll biomass, this implies that 32% of the diatom production (Feb. 24–March 11) had been 'lost', either to grazing or sedimentation. Second, an average phytoplankton assimilation efficiency of 6.7 μg C (μg chlorophyll)$^{-1}$ during Feb. 24–March 11 equals an average growth rate of 0.15 d^{-1} (C:Chl = 45). Together with the rate of net chlorophyll biomass increase (0.1 d^{-1}) this implies a phytoplankton loss rate of 33%.

A plot of cumulated sedimentation as % of cumulated primary production during the observation period (Fig. 15) shows that until March 11, sedimentation amounts to ca. 50% of primary production. Given the uncertainty in production and other estimates, this is consistent with the Silica budget and the phytoplankton growth and net accumulation rates given above. Thus, until March 11 sedimentation of resuspended matter is of secondary importance. Between March 11 and 16, during a period of very strong winds, cumulated sedimentation significantly exceeded primary production; this suggests significant sedimentation of resuspended matter during this period.

b. Significance of aggregate formation by coagulation

i. Coagulation of suspended particles. The main purpose of this study has been to investigate whether classical coagulation theory and flocculation of suspended

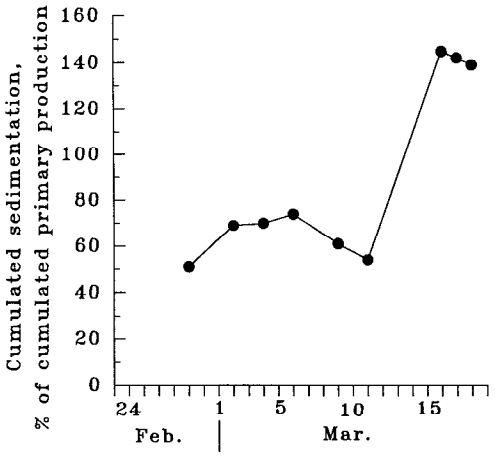

Figure 15. Cumulated sedimentation of particulate organic carbon as a function of cumulated primary production during the observation period.

particles into rapidly sinking aggregates can account for the observed pattern of sedimentation and, in particular, sinking velocity of suspended particulate material. To examine this we designed a predictor of flocculation ('flocculation potential') as the estimated flocculation index multiplied by the observed volume concentration of suspended particles in the water column and the estimated fluid shear rates. To make this predictor comparable to sedimentation and sinking rates provided by LTD, we averaged observations taken at the start and at the end of trap deployments.

In Figure 16 we compare observed sinking rates of particulate matter, sedimentation rates of aggregates and predicted flocculation. In qualitative terms there is a good correspondence between predicted aggregation and observed fall velocities of suspended particles. This pattern also resembles that of the sedimentation rate of aggregated material, thus supporting the prediction that elevated fall velocities are caused by aggregate formation. Thus, particle aggregation and classical coagulation theory appears to successfully predict observed sedimentation patterns.

However, the observed pattern in sedimentation and sinking may be partly due to resuspension of 'heavy' and rapidly sinking particles following wind events. Wind generated turbulence will also enhance collision rates between suspended particles and, hence, predicted flocculation, and one cannot with certainty distinguish the two processes. The considerations above suggest that the high sedimentation rates during March 11–16 were to a large extent due to sedimentation of resuspended bottom material. However, the elevated sinking velocities of individual algal species and of particulate chlorophyll, both during this period and during March 2–4, can best be explained by aggregate formation, whether the aggregating particles were of genuine

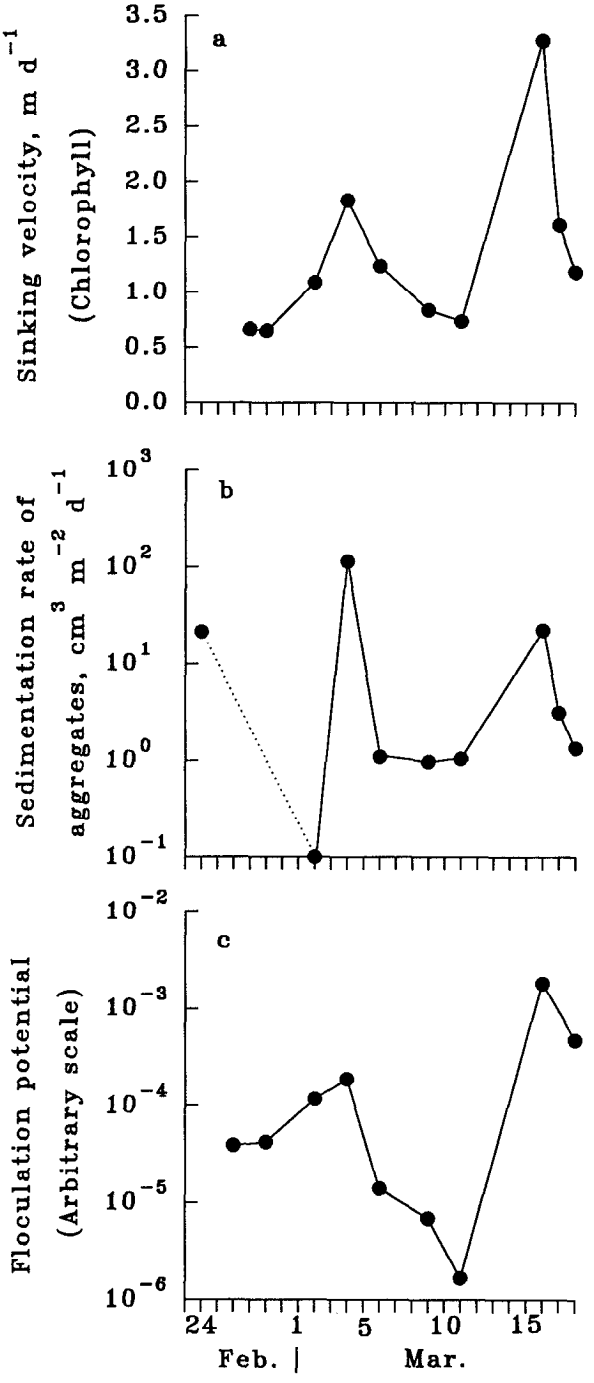

Figure 16. Observed sinking velocity of particulate chlorophyll *a* in LTD traps (a), observed sedimentation rate of aggregates (detritus- and algal aggregates) in STD traps (b) and rate of aggregate formation ('flocculation potential') predicted from coagulation theory (c) during the observation period.

planktonic or benthic origin. This is supported by the temporal variation in sedimentation of aggregated material and suggests that aggregation does play a major role.

ii. Coagulation of phytoplankton. Above we have discussed coagulation of particulate material without distinguishing between types of particles. In the following we apply coagulation theory more specifically to the phytoplankton. By combining coagulation theory and algal growth dynamics Jackson (1990) showed that:

$$dC/dt = \mu C - 2.608\alpha\gamma C^2 d^3,$$

where C is the concentration of single cells, μ is the net algal growth rate (i.e. growth—grazing—sedimentation of uncoagulated cells), and d the cell diameter. For simplicity only collisions between single cells are considered, because these dominate the coagulation process. The validity of this simple model has been confirmed by more elaborate models of Jackson and Lochmann (1992). According to this model the phytoplankton population will initially grow exponentially and subsequently approach an equilibrium concentration (critical concentration, C_{cr}) where growth and coagulation (and subsequent sedimentation) balances. The development of the populations of the 5 dominant species of phytoplankton all fit this pattern (Fig. 8). Also, the synchronized decline in cell concentrations subsequent to a period of elevated fluid shear rates March 2–4, accords with the model. The implicit assumption, that μ is constant throughout, is supported by the constant assimilation efficiency of the phytoplankton, and the unlimiting concentrations of inorganic nutrients during the observation period. The critical cell concentration (C_{cr}) can be estimated by putting $dC/dt = 0$:

$$C_{cr} = 0.384\mu(\alpha\gamma d^3)^{-1}.$$

The critical concentrations predicted by this model were calculated assuming $\gamma = 1.2\ s^{-1}$ (the average shear during the study period), μ = initial exponential growth rate for each species (Table 2), and d = the maximum linear cell dimension (except for *Rhizosolenia hebetata* where we used the equivalent spherical diameter). For simplicity we further assume $\alpha = 1$ for all species, but we elaborate on this below. This analysis is crude, in that we ignore that some species are chainforming and possess extrusions, thus to some extent changing the effective cell size. Yet, predicted critical and maximally observed concentrations during the study period compare to within one order of magnitude over a 4 order of magnitude variation in cell concentration (Fig. 17 and Table 2; see also Fig. 8).

We also did the inverse analysis, by putting C_{cr} = observed max. Cell concentration and solving for α. The estimated stickiness coefficients required to obtain the observed cell concentrations have been given in Table 3. Estimated α for *Skeletonema costatum* compares well with what we have measured in the laboratory for this species (Kiørboe *et al.*, 1990; Kiørboe and Hansen, 1993; Drapeau *et al.*, 1994), α for

Table 2. Cell sizes, initial net population growth rates, maximal cell concentrations and estimated critical concentrations (*sensu* Jackson, 1990) for 5 species of diatoms in the Isefjorden during February 24–March 18. Population growth rates have been calculated from changes in cell concentrations on the first 3 or 4 observation days. Cell sizes are maximum linear dimensions, except for *Rhizosolenia hebetata* where it refers to the equivalent spherical diameter.

Species	Growth rate (μ), d^{-1}	Cell size (d), μm	Maximal cell concentration, ml^{-1}	Critical concentration (C_{cr}), ml^{-1}
Skeletonema costatum	0.43	7.63	10^4	3.58×10^3
Thalassiosira spp.	0.37	23.0	5.5×10^1	1.13×10^2
Leptocylindrus danicus	0.54	17.27	1.5×10^2	3.88×10^2
Rhizosolenia hebetata	0.25	27.43	10^1	4.48×10^1
Coscinodiscus concinnus	0.33	250.0	10^0	7.80×10^{-2}

Coscinodiscus concinnus is realistic, while α for the three medium and similar sized species are all > 1. This simple model, thus, appears to underestimate collision rates for these species.

Jackson's (1990) model of critical concentration assumes a monospecific bloom. In the present case we have 5 diatom species that occur in significant concentrations simultaneously and we, thus, attempted a slightly more complex model approach by letting the species interact. As in Jackson we consider only collisions between single cells. The concentration of individual cells of the i'te species (C_i) changes according to (in analogy with Jackson, 1990):

$$dC_i/dt = \mu_i C_i - 2\, C_i \Sigma \alpha_{ij} C_j E_{ij} \beta_{ij},$$

where β is the coagulation kernel and E the contact efficiency. The parameters have been specified in Table 4. We here introduce the contact efficiency, E, which is the probability that two particles in close proximity come into direct contact. E is close to unity for like sized particles, and is included in α the way we estimate it experimentally for single species in the laboratory (Kiørboe *et al.,* 1990; Kiørboe and Hansen, 1993). However, it declines rapidly with increasing difference in the size of approaching particles (Hill, 1992; Riebesell and Wolf-Gladrow, 1992; Table 4). We also take differential settling into account, because we are now considering cells of different size and settling velocity simultaneously.

As above we put $dC_i/dt = 0$ and $C_{cr,i}$ = max. observed cell concentration of i'te species and solve for $\alpha_{11}, \alpha_{22}, \ldots, \alpha_{55}$, which are the stickiness coefficients required to obtain the observed cell concentrations (Table 3). The estimates compare well with those estimated in laboratory experiments for the same or for similar species (Kiørboe and Hansen, 1993). The negative estimates for some species presumably arise due to the way we calculate interspecific stickiness, but suggest that the

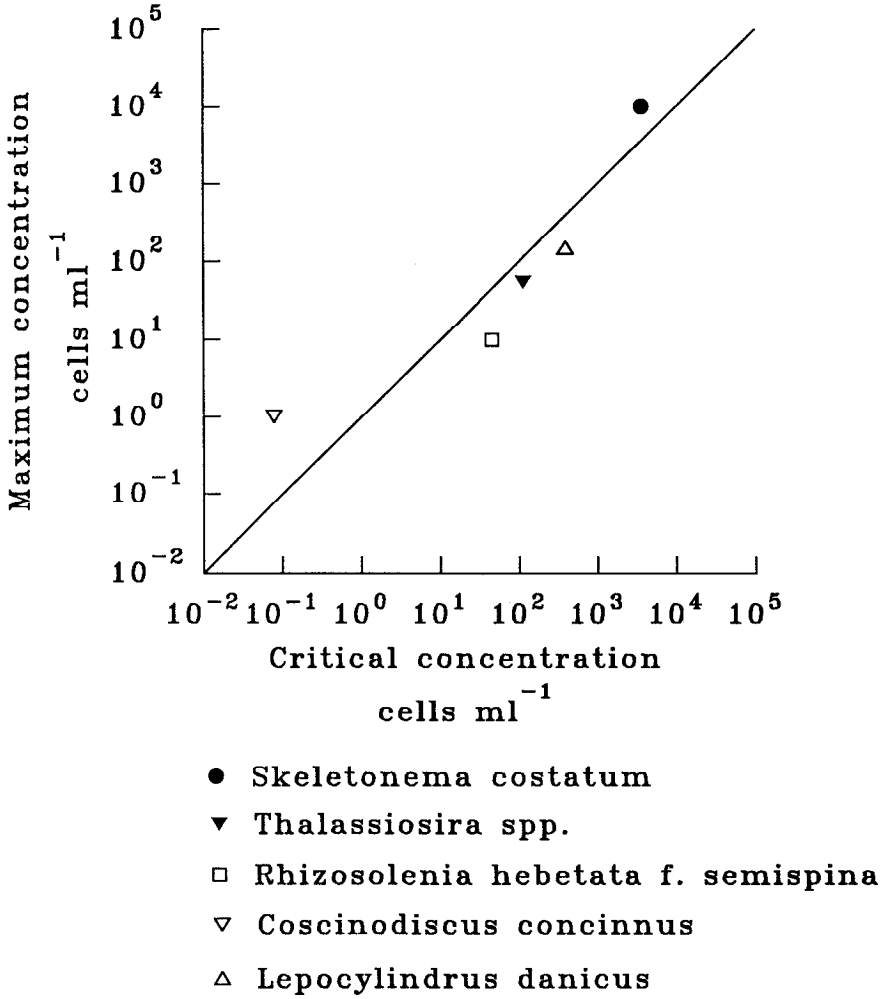

Figure 17. Maximum cell concentrations during the study period of the 5 dominating diatom species as function of the predicted 'critical concentrations' (*sensu* Jackson, 1990). The critical concentrations have been calculated assuming stickiness $\alpha = 1$, fluid shear rate $\gamma = 1.2\ s^{-1}$ and by using measured maximum dimensions of the cells (except for *Rhizosolenia hebetata*, where we used the equivalent spherical diameter) and measured initial population growth rates (see Table 2). The line is X = Y.

stickiness of these are low. We also did the calculation assuming that differential settling is zero (i.e. $\beta_{ij,\text{settling}} = 0$, Table 4). This does not change the α estimates much, indicating that the relative significance of differential settling in bringing particles to collide in this system is limited.

We have here shown that both phytoplankton and detritus form aggregates and that the dynamics of the bloom as well as the temporal pattern in aggregate

Table 3. Stickiness (α) required to yield observed cell concentrations of 5 species of diatoms calculated under various assumptions: (A) Monospecific blooms; the species do not interact; (B) Multispecies bloom with interspecific collisions and adhesion; collisions due only to turbulent shear; (C) as B but differential settling contributes also to cell collisions.

Species	Stickiness A: monospecies bloom; no interspecific interactions	Stickiness B: Multispecies bloom; only turbulent shear	Stickiness C: multispecies bloom; turbulent shear and differential settling
Skeletonema costatum	0.36	0.35	0.35
Thalassiosira spp	2.05	−0.08	−0.10
Leptocylindrus danicus	2.59	0.13	−0.10
Rhizosolenia hebetata	4.48	−0.18	−0.19
Coscinodiscus concinnus	0.08	−0.24	−0.25

sedimentation and particle sinking are largely consistent with coagulation theory. However, we have been unable to decide what binds particles together. Recently Alldredge *et al.* (1993) described the occurrence of large transparent exopolymer particles (TEP) in high concentrations (30–5000 ml^{-1}) in the sea off California. These particles, presumably of phytoplankton origin, may add to the volume of suspended particles and thus increase interparticle collision frequency, but can be

Table 4. Definition of model parameters.

$\beta_{ij}E_{ij} = (\beta_{ij,\text{shear}}E_{ij,\text{shear}}) + (\beta_{ij,\text{settling}}E_{ij,\text{settling}})$

$\beta_{ij,\text{shear}} = 1.3\gamma(r_i + r_j)^3$

$\beta_{ij,\text{settling}} = 2.48\pi(r_i + r_j)^3|r_i^{1.17} - r_j^{1.17}|$ (Hill, 1992; Jackson 1990)

$E_{ij,\text{shear}} = 7.5p^2(1 + 2p)^{-2}$ for $i \neq j$ (Hill, 1992)

$E_{ij,\text{shear}} = 1.0$ for $i = j$ (because already included in α the way we estimate it)

$E_{ij,\text{settling}} = 0.5p^2(1 + p)^{-2}$

$p = d_i/d_j$ $(d_i < d_j)$

$\alpha_{ij} = \alpha_{ji} = 0.5(\alpha_{ii} + \alpha_{jj})$ (We thus assume that the stickiness coefficient between two species is the average of the individual stickiness coefficients.)

γ = shear rate = 1.2 s^{-1} (average shear rate during observation period)

d_i = diameter of i'te species

quantified only by staining techniques; they are not sensed by electronic particle counter. Passow *et al.* (1994) and Kiørboe and Hansen (1993) showed that diatom-produced TEP may act to bind non-sticky particles together and Alldredge *et al.* (1993) suggested that TEP may play a major role in marine snow formation in the ocean. However, the simple coagulation model considered above appear to be able to account for phytoplankton bloom dynamics and phytoplankton aggregate formation without invoking the existence of TEP or other hydrosols (cf. also Hill, 1992). This bloom was numerically dominated by *Skeletonema costatum* which species Kiørboe and Hansen (1993) showed would coagulate without involving TEP. There are several other reports that *S. costatum*-dominated blooms are terminated by aggregate formation and sedimentation (e.g. Bodungen *et al.,* 1981; Riebesell, 1989; 1991b; Olesen, 1993), and in all of these cases available information about wind speed or turbulence and maximally observed cell concentrations are consistent with critical concentrations calculated from Jacksons (1990) model (see also below). TEP may still have played a role in these systems but may be particularly significant for particle coagulation in systems not dominated by *S. costatum.* For example, the abundant occurrence of aggregates in regions where particle concentration is low and models predict coagulation to be insignificant, e.g. during summer in the nearby Kattegat (Olesen and Lundsgaard, 1993), may be explained by the occurrence of TEP.

While several theoretical models describing coagulation of phytoplankton have been developed recently (Jackson, 1990; Jackson and Lochmann, 1992, 1993; Hill, 1992; Riebesell and Wolf-Gladrow, 1992), there are few attempts to rigorously test their predictions in the field. Weilenmann *et al.* (1989) combined modelling with field observations of sedimentation rates and stickiness of naturally occurring particles in Lake Zürich and concluded that coagulation was important and could account for observed vertical particle fluxes. Riebesell (1991a,b) in his study of a diatom bloom in the North Sea found that the concentration of phytoplankton aggregates varied nonlinearily with phytoplankton concentration. This verifies the prediction of Jackson's (1990) coagulation model, showing aggregate formation to be a two state system, where coagulation is unimportant at low and dominant at high cell concentrations, and with a rapid transition between the two states. Riebesell (1991b) also applied Jackson's 'critical concentration equation' in an attempt to explain maximum observed diatom concentrations. However, the model overestimated the critical concentration by an order of magnitude. However, Riebesell assumed a phytoplankton growth rate of 1 d^{-1}, while the initial exponential net growth rate of individual species in his study varied between 0.04–0.27 d^{-1} and averaged 0.15 d^{-1} (calculated from his Fig. 3). With the lower growth rate of 0.15 d^{-1} observed and predicted cell concentrations come to within a factor of 2.

In conclusion, then, coagulation theory appears to account for significant properties of the dynamics and sedimentation of diatom blooms. Other groups of phytoplank-

ters are known to sink as aggregates, e.g. coccolithophorids (Honjo, 1982; Cadée, 1985), cyanobacteria (Lochte and Turley, 1988) and possible prymnosiophytes (Wassmann *et al.,* 1990), but the stickiness of these groups have not as yet been documented. Also, coagulation theory has not yet been specifically applied to or tested for these groups, some of which dominate the phytoplankton in large regions of the ocean.

Acknowledgments. Thanks are due to Janne Ravensholt, Jack Melbye, Inger Hornum, Esben Vedel Nielsen, Merete Allerup and Susanne Simonsen for technical assistance, to Benly Thrue and Bent Jørgensen of R/V *Ophelia* for assistance at sea and to Ken Cornelisse for preparing the graphs. We are grateful to Alice Alldredge, Hans Dam and George Jackson for critically reading earlier versions of the manuscript. This work was supported by grants from the Danish Science Research Council (Contract no. 11-0420-1), The National Agency of Environmental Protection in Denmark (Contract nos. HAV-90, 2-30 and 2-31) and from the U.S. Office of Naval Research (Contract no. N00014-93-1-0226).

REFERENCES

Alldredge, A. L. and C. Gotschalk. 1989. Direct observations of the flocculation of diatom blooms: characteristics, settling velocities and formation of diatom aggregates. Deep-Sea Res., *36,* 159–171.

Alldredge, A. L., U. Passow and B. E. Logan. 1993. The abundance and significance of a class of large, transparent organic particles in the ocean. Deep-Sea Res., *40,* 1131–1140.

Anon. 1973. Roskilde Fjords og Isefjords vandskifte. [Water residence times in Roskilde Fjord and Isefjord]. Report from the Danish Hydraulic Institute, 22 pp.

—— 1989. Undersøgelser af Isefjordens forureningstilstand i 1986 og 87/88. [Investigations of the pollution of Isefjord in 1986 and 1987/88]. Report, County of Vestsjælland, 127 pp.

Bodungen, B. V., K. V. Brockel, V. Smetacek and B. Zeitzschel. 1981. Growth and sedimentation of the phytoplankton spring bloom in the Bornholm Sea (Baltic Sea). Kieler Meeresforsch., S.h. *5,* 49–60.

Cadée, G. C. 1985. Macroaggregates of *Emiliana huxleyi* in sediment traps. Mar. Ecol. Prog. Ser., *24,* 193–196.

Camp, T. R. and P. C. Stein. 1943. Velocity gradients and internal work in fluid motion. J. Boston Soc. Civ. Eng., *30,* 219–237.

Drapeau, D. T., H. G. Dam and G. Greneier. 1994. An improved flocculator design for use in practical aggregation experiments. Limnol. Oceanogr. (in press)

Duuren, F. A. van. 1968. Defined velocity gradient model flocculator. J. San. Eng. Div. Proc. Am. Soc. Civ. Eng., *94 (SA4),* 671–682.

Edler, L. (ed.). 1979. Recommendations on methods for marine biological studies in the Baltic Sea. Phytoplankton and chlorophyll. Baltic Mar. Biol. Publ., *5,* 1–38.

Hill, P. S. 1992. Reconciling aggregation theory with observed vertical fluxes following phytoplankton blooms. J. Geophys. Res., *97,* 2295–2308.

Honjo, S. 1982. Seasonality and interaction of biogenic and lithogenic particle flux at the Panama Basin. Science, *218,* 883–884.

Jackson, G. A. 1990. A model of the formation of marine algal flocs by physical coagulation processes. Deep-Sea Res., *37,* 1197–1211.

Jackson, G. A. and S. E. Lochmann. 1992. Effect of coagulation on nutrient and light limitation of an algal bloom. Limnol. Oceanogr., *37,* 77–89.

——. 1993. Modelling coagulation of algae in marine ecosystems, *in* Environmental particles, J. Buffle, ed., *2,* 373–399.

Jannasch, H. W., O. C. Zafiriou and J. W. Farrington. 1980. A sequencing sediment trap for time-series studies of fragile particles. Limnol. Oceanogr., *25,* 939–943.

Jespersen, A. and K. Christoffersen. 1987. Measurements of chlorophyll *a* from phytoplankton using ethanol as extraction solvent. Arch. Hydrobiol., *109,* 445–454.

Kiørboe, T., K. P. Andersen and H. Dam. 1990. Coagulation efficiency and aggregate formation in marine phytoplankton. Mar. Biol., *107,* 235–245.

Kiørboe, T. and J. L. S. Hansen. 1993. Phytoplankton aggregate formation: observations of patterns and mechanisms of cell sticking and the significance of exopolymeric material. J. Plank. Res., *15,* 993–1018.

Kranck, K. and T. G. Milligan. 1988. Macroflocs from diatoms: *in situ* photography of particles in Bedford Basin, Nova Scotia. Mar. Ecol. Prog. Ser., *44,* 183–189.

Lochte, K. and C. M. Turley. 1988. Bacteria and cyanobacteria associated with phytodetritus in the deep sea. Nature, *333,* 67–69.

Lorenzen, C. J. 1967. Determination of chlorophyll and pheo-pigments: spectrophotometer equations. Limnol. Oceanogr., *12,* 343–346.

MacKenzie, B. R. and W. C. Legget. 1991. Quantifying the contribution of small-scale turbulence to the encounter rates between larval fish and their zooplankton prey: effects of wind and tide. Mar. Ecol. Prog. Ser., *73,* 149–160.

McCave, I. N. 1984. Size spectra and aggregation of suspended particles in the deep ocean. Deep-Sea Res., *31,* 329–352.

Olesen, M. 1993. The fate of an early diatom spring bloom. Ophelia, *37,* 51–56.

Olesen, M. and C. Lundsgaard. (1993). Seasonal sedimentation of autochthonous material from the euphotic zone of a coastal system. (submitted).

Passow, U., A. L. Alldredge and B. E. Logan. 1994. The role of particulate carbohydrate exudates in the flocculation of diatom blooms. Deep Sea Res., (in press).

Riebesell, U. 1989. Comparison of sinking and sedimentation rate measurements in a diatom winter/spring bloom. Mar. Ecol. Prog. Ser., *54,* 109–119.

—— 1991a. Particle aggregation during a diatom bloom. I. Physical aspects. Mar. Ecol. Prog. Ser., *69,* 273–280.

—— 1991b. Particle aggregation during a diatom bloom. II. Biological aspects. Mar. Ecol. Prog. Ser., *69,* 281–291.

Riebesell, U. and D. A. Wolf-Gladrow. 1992. The relationship between physical aggregation of phytoplankton and particle flux: a numerical model. Deep-Sea Res., *39,* 1085–1102.

Smetacek, V. S. 1985. Role of sinking in diatom life-history cycles: ecological, evolutionary and geological significance. Mar. Biol., *84,* 239–251.

Smoluchowski, M. 1917. Versuch einer matematischen Theorie der Koagulationskinetic kolloider Lösungen. Z. Phys. Chem., *92,* 129–168.

Strickland, J. D. H. and T. R. Parsons. 1968. A practical handbook of seawater analysis. Bull. Fish. Res. Bd. Can., *167,* 1–311.

Wassmann, P., M. Vernet, G. Mitchell and P. Rey. 1990. Mass sedimentation of *Phaeocystis pouchetti* in the Barents Sea during spring. Mar. Ecol. Prog. Ser., *66,* 183–195.

Weilenamnn, U., C. R. O'Melia and W. Stumm. 1989. Particle transport in lakes: models and experiments. Limnol. Oceanogr., *34,* 1–18.

Wintermans, J. F. G. M. and A. De Mots. 1965. Spectrophotometric characteristics of chlorophylls *a* and *b* and their phaeophytins in ethanol. Biochim. Biophys. Acta, *109,* 448–453.

Received: *5 July, 1993;* revised: *8 October, 1993.*